INSTITUTE OF PHYSICS PUBLISHING PLASMA SOURCES SCIENCE AND TECHNOLOGY

Plasma Sources Sci. Technol. **13** (2004) 359–370 PII: S0963-0252(04)78818-0

Parallel velocity and temperature of argon ions in an expanding, helicon source driven plasma

Xuan Sun, Costel Biloiu, Robert Hardin and Earl E Scime

Department of Physics, West Virginia University, Morgantown, WV, 26506, USA

Received 12 December 2003
Published 10 May 2004
Online at stacks.iop.org/PSST/13/359
DOI: 10.1088/0963-0252/13/3/001

Abstract
The parallel ion flow in a high-density helicon source plasma expanding into a region of weaker magnetic field is measured as a function of neutral pressure, magnetic field strength, rf power and rf driving frequency. The dependence of the parallel ion flow and parallel ion temperature, measured by laser induced fluorescence, on the plasma density, electron temperature and floating potential, measured with an rf-compensated Langmuir probe, is also examined. At the end of the helicon plasma source, the ion velocity space distribution changes from a single subsonically drifting Maxwellian population to a supersonic ion beam ($\approx$15 eV) plus a cold, subsonically drifting background ion population. At 38 cm into the expansion region beyond the end of the plasma source, the supersonic ion beam is not observed.

1. Introduction

Investigations of high-density plasmas expanding into a vacuum or into a low-density background plasma date back to the 1930s, when researchers observed high-velocity plasma jets in low-pressure dc discharges [1, 2]. Later experiments demonstrated acceleration of ions to supersonic speeds during plasma expansion [3–5], and some researchers have reported detailed measurements of both electron and ion velocity distribution functions from the expansion process in a pulsed plasma [6–8]. As discussed in [8], the physics of expanding plasmas plays a key role in a wide range of phenomena: in the filling of the wake region behind objects moving supersonically through a plasma [9]; in laser-fusion experiments where the laser heated target material expands away from the target [10]; and in the expansion of ionospheric plasma into the magnetosphere along the earth's magnetic field [11]. Laboratory experiments designed to probe the details of expanding plasmas have employed pulsed plasma sources [6–8], Q-machines with shaped magnetic fields [12, 13] and triple plasma devices [14, 15]. Interest in controlling the characteristics of expanding plasmas has been on the rise as expanding plasmas have become more common in plasma processing systems and plasma thrusters.

The high plasma densities and the possibility of either supplying an independent bias to the sample substrate or allowing the sample to float electrically makes helicon sources potentially attractive plasma processing sources. Typically, the sample to be processed is placed into a diffusion chamber connected to the helicon source. The plasma then expands from the strong magnetic field region of the source into the weaker magnetic field of the diffusion chamber. For materials processing applications involving deposition, surface modification or etching, control of the ion temperature, ion speed, plasma density and uniformity in the expanding plasma is of paramount importance. Researchers have shown that in the diffusion chamber, charge-exchange collisions associated with plasma expansions reduce the average energy of the ions impinging on a substrate. Thus, by operating at neutral pressures of several milliTorr, helicon plasma sources have been used for generating uniform plasma fluxes with a high plasma density and reduced ion energies at the substrate location in the diffusion chamber [16–18]. Arrays of compact helicon plasma sources have also been shown to produce uniform plasmas over large surface areas [19]. For plasma etching, high etching rates (1.5 μm min^{-1}) with a minimum anisotropy of 0.97 were obtained with an expanding SF_6 helicon plasma [20]. Control of both ion flow speed and ion temperature in the expanding plasma would provide important additional capabilities in a helicon source based etching system.

For plasma thrusters, the ion flow speed in the expanding plasma is the critical parameter. In a thermal plasma

thruster, the plasma is heated and the random energy of the hot propellant converted into directed flow, i.e. thrust, in a physical or magnetic nozzle [21–23]. Their high efficiency, compatibility with low mass ions for high specific impulse operation, steady-state operation without electrodes and modest magnetic field strengths make helicon plasma sources ideal candidates for thermal plasma propulsion systems. Since a magnetic nozzle is essentially an expanding magnetic field, control of the ion physics in the expanding plasma is critical to optimizing the characteristics of the plasma thruster.

We first reported significant, but subsonic, parallel ion flows in an open-ended helicon plasma source some years ago [24]. Even faster flows have been reported in other helicon sources [22], and ion flows have been studied in a variety of other expanding plasmas driven by electron cyclotron resonance [25, 26] and other plasma sources. However, two recent, independent experiments have sparked renewed interest in bulk ion flows in helicon sources by suggesting that supersonic, parallel ion flows in low pressure helicon source plasmas expanding into a region of decreasing magnetic field strength result from the formation of an electric double layer near the junction between the helicon source chamber and the expansion chamber. Because these experiments were performed in helicon sources, there was no externally imposed current or electron beam in the plasma—typically required to form a double layer in a laboratory plasma.

Charles and Boswell [27] have reported measurements of a discontinuity in the plasma potential, an electric double layer, at the end of the helicon source in a low pressure ($\leqslant$0.5 mTorr) helicon plasma. Using a retarding field energy analyser, they mapped the plasma potential along the axis of the device and found that when the neutral pressure dropped below 0.5 mTorr, a 'rapid and discontinuous change in the plasma potential close to the exit of the source' appeared. Of particular relevance to the experimental measurements that we will present in this paper, as the neutral pressure in the source was decreased from 3 to 0.2 mTorr, the electric field inside the source increased from approximately 50 to 220 V m^{-1}. The total potential drop from the closed end of the source to near the open end of the helicon source was approximately +50 V, equivalent to the acceleration of an argon ion at rest to a velocity of 15 500 m s^{-1}. Beyond the end of the helicon source, the plasma potential decreased only slightly. Given the measured electric fields, it was assumed that ions inside the source were accelerated out of the source and into the diffusion chamber. Very recent retarding potential analyser measurements in the same system have confirmed that ions are accelerated through the double layer structure in both argon [28] and hydrogen [29] plasmas.

Cohen *et al* [30] have reported measurements of supersonic ion flows emanating from a small aperture placed at the end of a low-pressure, high-power density helicon plasma source with a magnetic nozzle. In these experiments, a population of ions flowing out of the aperture at supersonic speeds was observed at low neutral pressures—independent of the magnetic nozzle field strength. The experiments of Cohen *et al* were performed at a helicon source neutral pressure of 0.5 mTorr. The maximum ion energy observed, 30 eV, corresponded to an ion flow speed of roughly 12 000 m s^{-1}, i.e. a specific impulse, I_{sp} ($\equiv v/g$, where $g = 9.8\,\mathrm{m\,s^{-2}}$), of 1200 s. The ion flow speed was measured with a tunable diode laser based laser induced fluorescence (LIF) diagnostic [31]. Inside the source chamber, ion flows at or below the ion thermal speed were observed. Based on the rapid acceleration of the ion flow in the vicinity of the aperture, within a few centimetres, it was suggested that an electric double layer was responsible for the observed ion acceleration.

In this paper, we present measurements of argon ion acceleration inside a large-volume, moderate-pressure expanding helicon plasma. The parallel ion flow and parallel ion temperature are measured by LIF, the plasma density, electron temperature and floating potential are measured using an rf-compensated Langmuir probe. The effects of the rf driving frequency, rf power, helicon source magnetic field and expansion chamber magnetic field on ion parallel flow at different locations are investigated. The principal result is the observation, at the end of the helicon plasma source, of two distinct ion groups: a supersonic ion beam ($\approx$15 eV) and a subsonically drifting background ion population. The relationship between plasma density, electron and ion temperature, floating potential in the helicon source and expansion chamber, and the parallel ion flow into the expansion chamber is also examined. We conclude with an analysis of our measurements in light of the observations of Charles and Boswell and Cohen *et al*.

2. Experimental apparatus

The HELIX (Hot hELIcon eXperiment) (figure 1) vacuum chamber is a 61 cm long Pyrex tube 10 cm in diameter, connected to a 91 cm long stainless steel chamber that is 15 cm in diameter. The stainless steel chamber has one set of four 6″ Conflat^{TM} crossing ports in the centre of the chamber and two sets of four $2\frac{3}{4}$″ Conflat^{TM} crossing ports on either side that are used for diagnostic access. The opposite end of the stainless steel chamber opens into a 2 m diameter, 4 m long aluminium chamber called Large Experiment on Instabilities and Anisotropies (LEIA) [24]. A common electrical ground is used for the vacuum chambers and the rf amplifiers, and all measurements are referenced to the chamber potential. Ten electromagnets produce an axial magnetic field of 0–1200 G in the source, and seven additional electromagnets generate an axial magnetic field in LEIA of 0–80 G. The source gas is

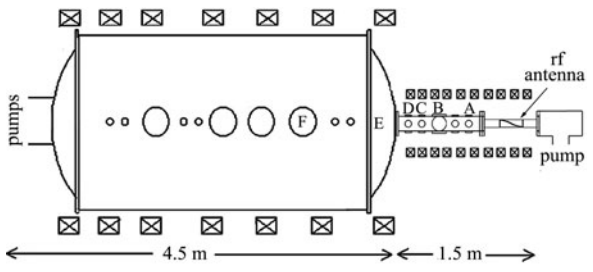

Figure 1. The HELIX–LEIA system. The 19 cm helical antenna is wrapped around the outside of the Pyrex section of the HELIX chamber between $z = 27$ and 46 cm from the right end of the source. LIF measurements were made at positions A, B, C and D in HELIX and along the axis of the LEIA chamber from position E to position F. Langmuir probe measurements were made at positions C and E through F. The labelled locations correspond to distances of (A) $z = 80$ cm, (B) $z = 111$ cm, (C) $z = 126$ cm, (D) $z = 146$ cm, (E) $z = 188$ cm and (F) $z = 272$ cm.

typically argon at neutral pressures of 1.0–20 mTorr. In the source, the gas pressure is measured on both sides of the rf antenna (figure 1), and in LEIA, the pressure is measured at both ends of the chamber. In LEIA, we find that the neutral pressure is uniform throughout most of the chamber. In the source, there is a pressure gradient along the axis of the system. rf power of up to 2.0 kW over a frequency range of 6–18 MHz is used to create the steady-state plasma. A 19 cm, half wave, $m = +1$ helical antenna couples the rf energy into the plasma [32]. Characteristic electron temperatures and densities in HELIX are $T_e \approx 4$–12 eV and $n \approx 2 \times 10^{11}$ to 1×10^{13} cm^3 as measured with an rf compensated Langmuir probe [33] and swept frequency microwave interferometer [34].

Vacuum pumping is accomplished through three turbomolecular drag pumps: a 540 litre s^{-1} pump at one end of HELIX and two 1600 litre s^{-1} pumps at the other end of LEIA. Each pump has two speed settings and is mounted behind a gate valve. The base pressure is 8×10^{-8} Torr in LEIA and 9×10^{-8} Torr in HELIX. A precision mass flow controller regulates the argon, helium or mixed gas flow rate. During operation, the neutral pressure in LEIA ranges from four to ten times lower than the pressure in the plasma source.

The magnetic field strength versus axial position (obtained from a two-dimensional code written specifically for the combined HELIX–LEIA system) is shown in figure 2(*a*) for typical operating parameters. Compared with Hall probe measurements at multiple axial and radial locations, the code is accurate to within a few per cent. Figure 2 is representative

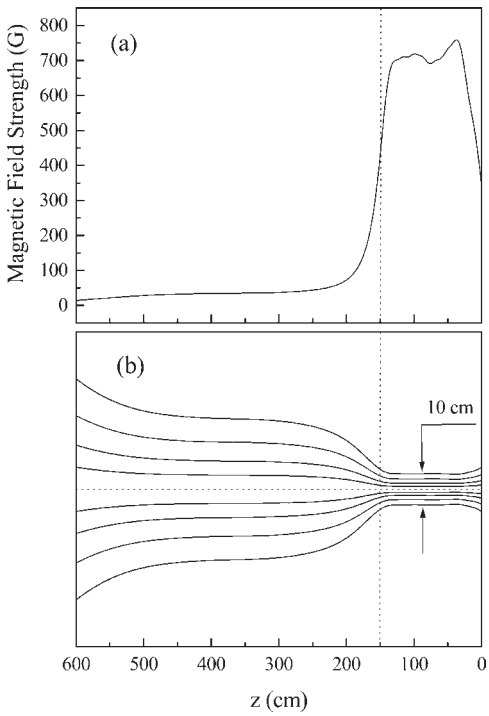

Figure 2. (*a*) Axial magnetic field strength versus axial position in the combined HELIX–LEIA system. The inhomogeneity in the magnetic field between 25 and 50 cm is due to displacement of the coils by the feeds for the rf antenna. (*b*) Contours of constant magnetic flux versus axial position. The outermost contours correspond to the plasma boundary in the source. The dashed vertical lines indicate the junction between the source chamber and the diffusion chamber.

of the magnetic field configuration used in most of the experiments presented in this paper. In figure 2(*a*), the 730 G axial magnetic field in HELIX drops to 70 G in LEIA over 0.7 m: a field gradient of nearly 1000 G m^{-1}. Contours of constant flux versus axial position are shown in figure 2(*b*) for the same parameters as in figure 2(*a*). Note that the field expansion begins inside the source vacuum chamber. By holding the source (HELIX) magnetic field strength fixed and varying the LEIA (source) magnetic field, the expansion gradient can be changed for fixed source parameters.

Measurements of the ion velocity space distribution function (ivdf), both parallel and perpendicular to the magnetic field, are obtained with spatially resolved, non-perturbative LIF [35–37]. The LIF laser system consists of a 6 W Coherent Innova 300 argon-ion laser that pumps a Coherent 899 tunable ring dye laser tuned to 611.49 nm. The 611.49 nm (air wavelength) photons pump the Ar II $3d^2G_{9/2}$ metastable state to the $4p^2F_{7/2}$ state, which then decays to the $4s^2D_{5/2}$ state by emitting 460.96 nm photons. As the laser frequency is varied over 20 GHz, the fluorescent emission from the pumped upper level is measured with a filtered (1 nm bandwidth around 461 nm) photomultiplier tube detector (PMT). A mechanical chopper operating at a few kilohertz is used to modulate the laser beam before it enters the vacuum chamber, and a Stanford Research SR830 lock-in amplifier is used to eliminate all non-correlated signals. After the laser light passes through the mechanical chopper, it is coupled into a multimode, non-polarization preserving fibre optic cable. The fibre optic cable transports the laser light from the laser laboratory into the helicon source laboratory, where several sets of laser injection and light collection optics are mounted on the HELIX and LEIA chambers. The collected fluorescence emission is also transported to the PMT by a fibre optic cable. Ten per cent of the laser output is passed through an iodine cell for a consistent zero velocity reference measurement to compensate for laser drift. Spontaneous emission from the iodine cell absorption lines is recorded with a photodiode for each scan of the dye laser wavelength.

For parallel injection of laser light (to measure the parallel ivdf), a linear polarizer–quarter wave plate combination is used to convert the unpolarized laser light exiting the fibre optic cable into circularly polarized light. With the laser light of a single circular polarization injected along the source axis, only one of the two σ transitions, specifically the $\Delta m = +1$ transition, is optically pumped. The much smaller internal Zeeman splitting of the different $\Delta m = +1$ σ lines is ignored during analysis of the parallel LIF data for magnetic field strengths less than 1000 G. Doppler broadening dominates the width of the measured ivdf, and the minimum resolvable ion temperature is 0.01 eV. The shift in the centre wavelength of the measured ivdf is used to determine the average flow of the ions along the laser path.

Collection optics spaced along the axis of the source (locations A, B, C and D in figure 1) and in LEIA (from E to F in figure 1) enable measurements of the parallel ivdf at different axial locations for the same plasma parameters. The collection optics in LEIA are mounted on a scanning probe assembly inserted from the side of the vacuum chamber at location F. The pivoting vacuum flange through which the probe is inserted permits a wide range of angular motion $\approx \pm 35^\circ$, and

incorporates additional linear and rotary motion feedthroughs [38]. For these experiments, the probe was configured to scan across a horizontal plane bounded along the axis by positions F and E as shown in figure 1. In addition to LIF injection and collection optics, the probe head includes an rf compensated Langmuir probe and a three-axis magnetic sense coil array. Position E is ≈38 cm from the end of the helicon source. The external collection optics at location D can be tilted to make parallel ivdf measurements from location D to the end of the source chamber.

A representative parallel LIF measurement with a corresponding iodine cell reference signal is shown in figure 3(*a*) for a nearly stationary plasma. The parallel drift velocity is determined from the shift of the LIF peak relative to the iodine signal minus the Zeeman shift of the σ absorption line. The experimental uncertainty in the ion flow speed is less than 50 m s^{-1}. A parallel LIF measurement of a rapidly drifting ion population with a background slowing drifting ion population is shown in figure 3(*b*).

We note in passing that although the LIF diagnostic is not absolutely calibrated, we have found that the total LIF signal is roughly proportional to the square of the plasma density times the square root of the electron temperature and can be used as a non-invasive measure of qualitative changes in the plasma density in argon helicon plasmas. Although the relationship between the total LIF signal and ion density is complex, if the metastable ions interrogated via LIF are created by electron impact excitation of ground state ions, the LIF signal intensity is roughly proportional to the square of the plasma density [39];

$$n^2 = n_i n_e \approx \frac{n_j}{\langle \sigma v \rangle_{0j}} \sum_{i<j} A_{ij} \tag{1}$$

where n is the plasma density, n_i the ion density, n_e the electron density, n_j the density of ions in the metastable state, j, probed with the laser (proportional to the total LIF signal), $\langle \sigma v \rangle_{0j}$ is the velocity distribution averaged cross section for electron impact excitation from the ion ground state into state j, and $\sum_{i<j} A_{ij}$ is the sum of the spontaneous transition rates from the metastable state to all lower states. The assumption that transitions from other metastable states are not significant sources of the interrogated metastable ions is equivalent to claiming that the ion state populations in argon helicon plasmas can be calculated with a steady-state coronal (SSC) model [40]. In support of this assertion, the LIF intensity in the helicon source as a function of rf driving frequency and radial position is compared with the square of the Langmuir probe measured plasma density times the square root of the electron temperature (as suggested by equation (1)) in figures 4(*a*) and (*b*), respectively. That the trends in the LIF and Langmuir probe measurements are remarkably similar indicates that LIF intensity measurements can be used as a qualitative measure of changes in the source plasma density. Perhaps more importantly, the similarity between the LIF

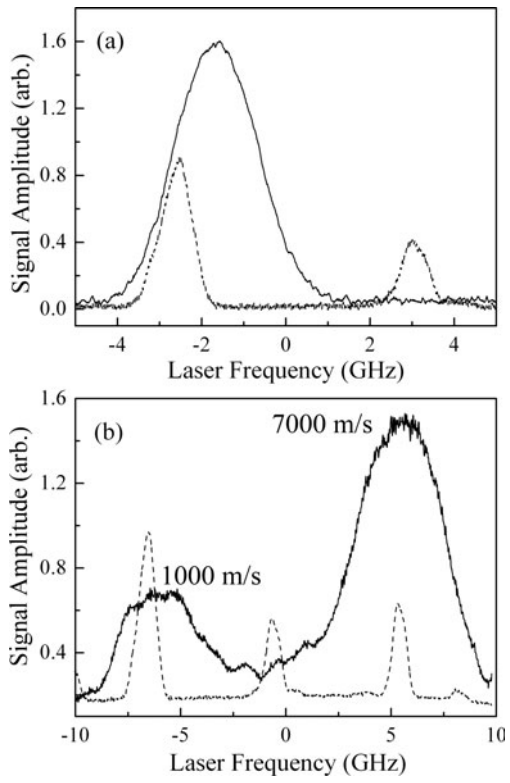

Figure 3. (*a*) Typical parallel ivdf measurement showing the Zeeman shifted Ar II $3d^2G_{9/2}$ to $4p^2F_{7/2}$ transition at 611.49 nm (——) and the reference iodine cell absorption line (- - - -). (*b*) A parallel ivdf measurement of a rapidly drifting ion population, $v \sim 7000$ m s^{-1}, with a background slowing drifting ion population obtained at the end of the helicon source (location D in figure 1). Note the different horizontal axis scales for the two figures.

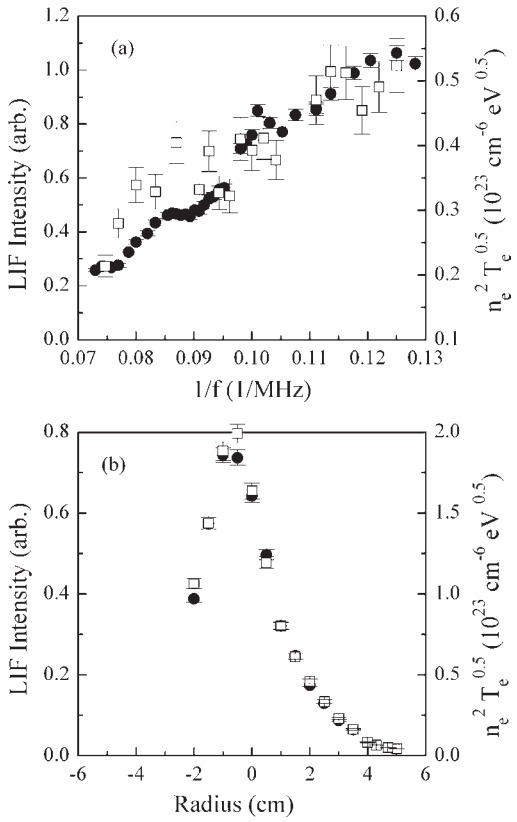

Figure 4. For an rf power of 750 W, $B_H = 730$ G and $B_L = 34$ G, the LIF intensity (●) and the square of the plasma density times the square root of the electron temperature (□) (*a*) versus inverse of the rf driving frequency and (*b*) versus radial position in HELIX. The frequency scan was performed at a neutral pressure of 1.2 mTorr and the radial scan at a neutral pressure of 1.8 mTorr.

and Langmuir probe measurements suggests that the high collisionality of high density argon helicon plasmas rapidly de-populates the ion metastable states and those metastable ions observed with LIF are locally and recently created via electron impact excitation of ground-state ions.

The plasma density, electron temperature and floating potential measurements were obtained at position C (see figure 1) using a radially scanning, rf compensated cylindrical Langmuir probe and from positions E to F with the rf compensated, cylindrical Langmuir probe mounted on the scanning probe assembly. It is well known that electron saturation is difficult to obtain with small cylindrical Langmuir probes in high-density plasmas [41]; thus we do not have direct measurements of the plasma potential in this paper. Instead, the argon plasma potential was estimated from measurements of the floating potential and the electron temperature according to [42, 43].

$$V_p = V_f + 5.4T_e, \tag{2}$$

where the factor of 5.4 depends on the logarithm of the ion-to-electron mass ratio.

3. Ion flow speed in the HELIX–LEIA system

The parallel ion flow velocity, parallel ion temperature and perpendicular ion temperature along the axis of the HELIX chamber were measured as a function of rf driving frequency, rf power, neutral pressure and magnetic field strength. Because recent measurements in HELIX demonstrated a clear correlation between power coupling into helicon plasmas (through ion heating and increased density) and a combination of rf driving frequency and magnetic field strength [44, 45], one objective of these experiments was to determine if the parallel ion flow varied with either rf driving frequency or magnetic field strength.

Significant electron temperature changes resulting from changing power coupling efficiencies and/or varying plasma densities are also expected to play an important role in ion acceleration through changing the ion sound speed and the potential gradients. Thus, the electron density, electron temperature and floating potential in the source and expansion chamber were also measured at several axial locations to gain insight about the influence of these plasma parameters on plasma flow.

3.1. Effects of rf driving frequency

The parallel ion speed and parallel ion temperature measured on axis at location C versus the rf driving frequency for an rf power of 750 W and a neutral pressure of 1.2 mTorr are shown in figure 5. The magnetic field in HELIX, B_H, was 730 G, and the lower hybrid frequency on axis $\omega_{LH} \approx \sqrt{\omega_{ce}\omega_{ci}} \approx 8$ MHz, where ω_{ce} and ω_{ci} are the electron and ion cyclotron frequencies, respectively. Since the plasma density decreases towards the edge of the source, the ion plasma frequency term in the full lower hybrid frequency calculation becomes significant and the lower hybrid frequency at the plasma edge is smaller than on axis [32]. Apart from a slight increase (≈10%) at rf driving frequencies just above the lower hybrid frequency on axis, the parallel ion flow speed of ≈1000 m s^{-1} and parallel ion temperature of 0.7 eV are independent of the rf

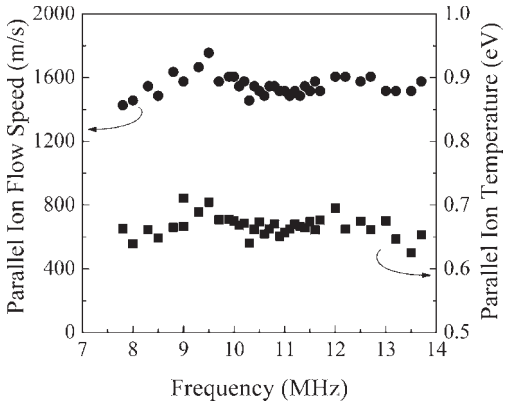

Figure 5. Parallel ion flow speed (●) and parallel ion temperature (■) versus rf driving frequency. The measurements were taken at location C (see figure 1) for a rf power of 750 W, $B_H = 730$ G, $B_L = 34$ G and neutral pressure of 1.2 mTorr in HELIX.

driving frequency. At higher neutral pressures (≈4 mTorr), the parallel ivdf is collisionally coupled to the perpendicular ivdf, and significant ion heating occurs for rf driving frequencies equal to the lower hybrid frequency at the plasma edge [45].

As already shown in figure 4(*a*), both the LIF intensity (estimated plasma density) and measured plasma density increase with decreasing driving frequency in these low pressure helicon discharges. The slight increase (decrease) in the LIF intensity (plasma density) for rf driving frequencies close to the lower hybrid frequency (ω_{LH}) on axis ($1/f \approx 0.11$ MHz^{-1}) is reminiscent of changes in the power coupling into the source observed at higher neutral pressures (≈4 mTorr) for $\omega \approx \omega_{LH}$ [32]. However, the overall inverse scaling of plasma density with rf driving frequency is only observed at low neutral pressures (<3 mTorr) and is consistent with the helicon wave dispersion relation. For a fixed magnetic field strength and fixed parallel and perpendicular wavelengths, the simple helicon wave dispersion relation for a homogeneous, small aspect ratio ($L \gg a$, where L is the length of the system and a is the plasma radius) helicon source [46],

$$n = \frac{B_0 k_{||}}{\omega \mu_0 e \alpha}, \tag{3}$$

predicts an inverse relationship between plasma density and rf driving frequency, where $\alpha(r)^2 = k_{||}^2 + k_\perp^2$, $k_{||}$ and $k_\perp$ are the parallel and perpendicular wave numbers, respectively, B_0 is the source magnetic field, μ_0 is the free space permeability, e is the electron charge and n is the electron density.

3.2. Effects of rf power

For a fixed rf driving frequency of 9.5 MHz and a source magnetic field of 730 G, the rf power was varied from 250 to 1000 W for two different neutral pressures: 1.2 and 1.7 mTorr as measured in the middle of the source chamber (corresponding to pressures of 2.0 and 3.1 mTorr at the gas inlet in the helicon source). The parallel ion flow speed was measured on the source axis at $z = 126$ cm (location C) for the 1.2 mTorr case and at $z = 146$ cm (location D) for the 1.7 mTorr case (figure 6(*a*)). In both cases and at both locations, there is a general trend of increasing flow speed with

increasing rf power. The parallel ion flow speed is roughly twice as fast near the end of the source as at $z = 126$ cm, even though the measurements at $z = 146$ cm were obtained at a much larger neutral pressure. Also shown in figure 6(*a*) is the parallel ion temperature versus rf power at $z = 126$ cm for the 2.0 mTorr case. The parallel ion temperature is nearly constant at roughly 0.7 eV until the rf power exceeds 600 W. Above 600 W, the parallel ion temperature rises to nearly 1.0 eV at an rf power of 800 W.

The square root of the LIF signal amplitude as a function of rf power is shown in figure 6(*b*). At both locations and at both pressures, the estimated plasma density (proportional to the square root of the LIF signal assuming a constant electron temperature) rises steadily with increasing rf power until a pressure dependent critical rf power is reached. In the 1.2 mTorr case, at location C, the plasma density stops increasing for rf powers greater than 600 W. Similar plateaux in measured plasma density have been observed in previous HELIX experiments [47]. At the higher neutral pressure, 1.7 mTorr, the plateau in estimated plasma density does not occur until the rf power reaches 800 W.

Note that in these measurements, the parallel ion flow speed at the upstream, $z = 126$ cm, location is much lower than the ion sound speed $C_s \approx 4500\,\mathrm{m\,s^{-1}}$ ($C_s = \sqrt{\gamma k T_e/m_i}$, where $\gamma = 1$ is assumed for isothermal expansion, k is Boltzmann's constant and m_i is the ion mass), while at the end of the source the parallel ion flow speed increases slightly with rf power and remains roughly equal to the ion sound speed throughout the rf power scan. In laboratory plasmas with an open magnetic field geometry, it is typically assumed that the electrons stream out along the magnetic field and the ions are dragged out at the ion sound speed by the ambipolar electric field [43]. However, ionization of neutrals along the axis of the system, radial transport, ion–electron recombination and neutral drag (due to ion–neutral collisions including charge-exchange) can all modify the ion flow along the magnetic field. In the case of a constant total ion flux along the axis of the system (arising perhaps from a plasma created upstream that then flows downstream without further ionization or recombination), as the surfaces of constant magnetic flux expand and the plasma density decreases, the parallel ion flow must increase. These measurements show clearly an increase in parallel ion flow speed as the ions enter the region of weakening magnetic field at the end of the helicon source—a substantial increase in parallel flow speed even though the further downstream measurements were made at a higher neutral pressure. The slight increase in parallel ion flow speed with increasing rf power could simply be due to the decrease in ion drag due to collisions with neutrals at higher rf powers. The drag due to neutrals decreases at the higher rf power powers because the plasma density increases (figure 6(*b*)) while the neutral pressure is held fixed, i.e. the neutral density decreases with increasing rf power.

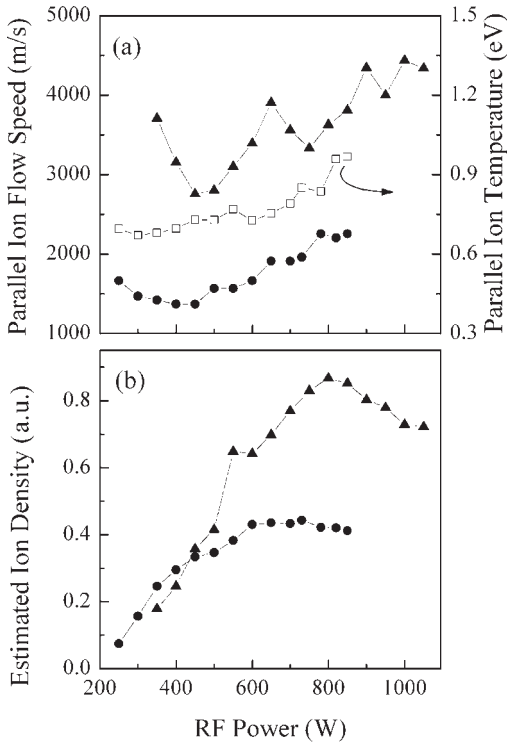

Figure 6. (*a*) Parallel ion flow speed in HELIX versus rf power for a neutral pressure of 1.2 mTorr at $z = 126$ cm (●) and 1.7 mTorr at $z = 146$ cm (▲). Also shown is the parallel ion temperature for a neutral pressure of 1.2 mTorr at $z = 126$ cm (□). (*b*) The ion density estimated from the LIF intensity versus rf power for a neutral pressure of 1.2 mTorr at $z = 126$ cm (●) and 1.7 mTorr at $z = 146$ cm (▲). For these measurements, $B_H = 730$ G and $B_L = 34$ G and the rf driving frequency was 9.5 MHz.

3.3. Effects of neutral pressure

By varying the number of active turbomolecular drag pumps, by operating the pumps at different rotation frequencies and by adjusting the input gas flow rate, the neutral pressure in LEIA was varied without altering the neutral pressure in HELIX or other source parameters. Figure 7 shows that the estimated plasma density measured in HELIX at $z = 126$ cm (location C) increases by approximately 10% for a 6% increase in the LEIA neutral pressure (from 0.13 to 0.14 mTorr). The HELIX neutral pressure remains fixed at 1.2 mTorr, while the LEIA pressure increases. Also shown in figure 7 is a roughly 10% decrease in parallel ion flow speed measured at location C in HELIX. Therefore, even a miniscule change in the downstream neutral

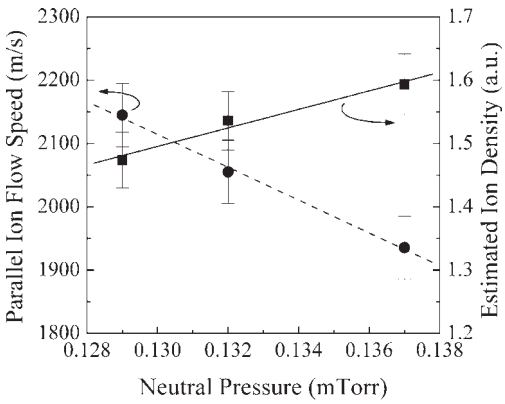

Figure 7. Parallel ion flow speed (●) and the ion density estimated from the LIF intensity (■) measured at location C in HELIX versus neutral pressure in LEIA for a fixed neutral HELIX pressure of 1.2 mTorr, $B_H = 730$ G, $B_L = 34$ G, rf driving frequency of 9.5 MHz and rf power of 750 W.

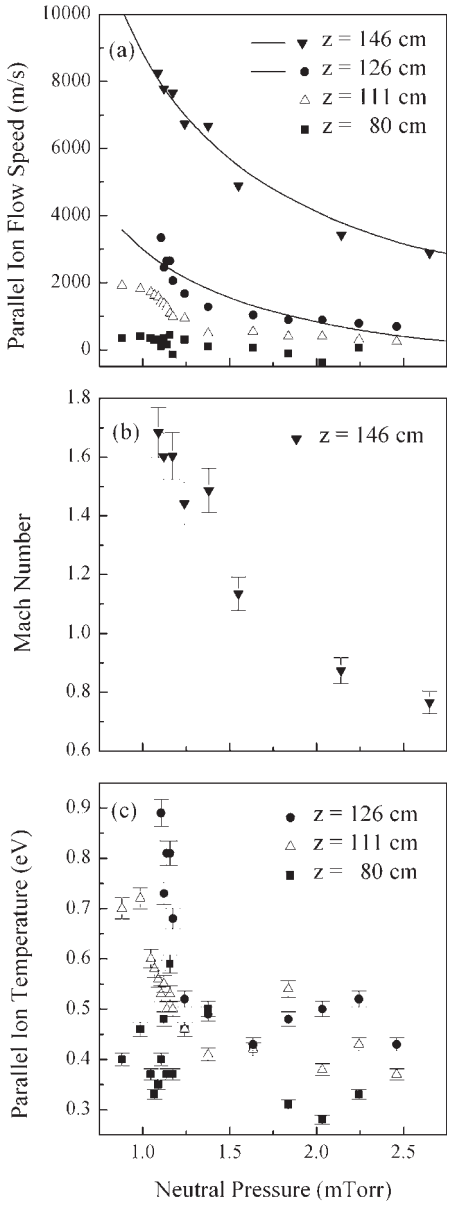

Figure 8. (*a*) Parallel ion flow speed, (*b*) Mach number and (*c*) parallel ion temperature measured at different locations in HELIX versus source neutral pressure for $B_H = 730$ G, $B_L = 34$ G, rf driving frequency of 9.5 MHz and rf power of 750 W. Solid lines are $v_{i||} = A/P_o + B$ fits to the measured parallel ion flow speeds.

pressure affects the parallel ion flow speed deep inside the helicon source.

The parallel ion flow speed and parallel ion temperature measured at four locations in the helicon source as a function of the neutral pressure in HELIX are shown in figure 8(*a*). Because the Zeeman shift could not be determined for the furthest downstream measurement at $z = 146$ cm (the uncertainty in the magnetic field strength was too large), unpolarized light is used for LIF measurements at that location and the parallel ion temperature is not determined. The parallel ion flow at $z = 146$ cm normalized to the ion sound speed in the source is shown in figure 8(*b*). Well inside the helicon source, $z = 80$ cm, there is little parallel ion flow, $v_{i||} \leqslant 300\,\mathrm{m\,s^{-1}}$. Further downstream, $z = 111$ cm, the parallel ion flow is somewhat larger, $v_{i||} \approx 400\,\mathrm{m\,s^{-1}}$ for neutral pressures greater than 1.2 mTorr. As the pressure drops below 1.2 mTorr, the parallel ion flow increases quickly to approximately $2000\,\mathrm{m\,s^{-1}}$ and then stays constant as the pressure is further reduced. Even further downstream, $z = 126$ cm, the parallel ion flow increases to nearly $4000\,\mathrm{m\,s^{-1}}$ at a neutral pressure of 1.1 mTorr. At 1.1 mTorr, the electron temperature in the source is roughly 10 eV, corresponding to an ion sound speed of $4900\,\mathrm{m\,s^{-1}}$ for argon ions. Thus, as can be seen in figure 8(*b*), the parallel ion flow close to the end of the helicon source and well within the magnetic field expansion region, $z = 146$ cm, is close to twice the sound speed, $v_{i||} \approx 8000\,\mathrm{m\,s^{-1}}$ ($1.7C_s$), at 1.1 mTorr. Ion beams with velocities of roughly $2C_s$ downstream of the double layer were also observed by Charles and Boswell in their most recent experiments [28].

Consistent with the experiments of Cohen *et al*, the rapidly flowing ion beam is one of two ion populations observed at the end of the helicon source at neutral pressures below 1.6 mTorr (see figure 3(*b*)). Both ion populations drift along the system axis towards the LEIA chamber. At $z = 146$ cm and for neutral pressures greater than 1.6 mTorr, only a single ion population is observed. In the experiments of Cohen *et al*, the two ion populations were found in the expansion region of the magnetic nozzle and downstream of a flux limiting aperture plate. Two ion populations, a 'passing' population and a 'trapped' population are characteristic of electric double layers [15]. There is no flux limiting aperture in these helicon experiments, nor is there a strong magnetic nozzle field. Thus, the formation of an ion beam, and by implication an electric double layer, inside the helicon source appears to be a general characteristic of these types of expanding, high-density plasmas. At the $z = 126$ cm location, there is also evidence of flow thermalization, probably by collisions, as the speed increases at low pressure (figure 8(*c*)). The parallel ion temperature increases 100% (from 0.5 to 1.0 eV) as the neutral pressure drops from 1.2 to 1 mTorr. Note that although we were unable to sustain stable helicon discharges at 0.6 mTorr, the neutral pressure at which strong double layer formation was observed in the other helicon source double layer experiments [27], the distinct change in source characteristics begins at a higher neutral pressure of 1.2 mTorr in these experiments.

The parallel ion flow measurements shown in figure 8(*a*) indicate a complex dependence of parallel ion flow on neutral pressure. Well inside the source, the parallel ion flow is relatively independent of neutral pressure until the pressure drops below 1.2 mTorr. Below 1.2 mTorr, the upstream parallel ion flow speeds increase sharply and, for the furthest upstream measurements, reach a plateau. However, the parallel ion flow speed at the end of the source appears to have a more simply defined dependence on neutral pressure. Note the lack of any threshold value of neutral pressure at which the parallel ion flow speed at $z = 146$ cm changes dramatically. Shown in figure 8(*a*) are fits to the two furthest downstream measurements. Each fit is of the form $v_{i||} = A/P_o + B$, and while the fit to $z = 126$ cm is poor, the fit to $z = 146$ cm measurements is excellent. Assuming for the moment that $z = 146$ cm parallel ion flow measurements reflect a balance between acceleration in an axial electric field and some sort of

drag process, the momentum balance equation,

$$m\frac{\mathrm{d}v_{\mathrm{i}||}}{\mathrm{d}t} = eE - \frac{mv_{\mathrm{i}||}}{\tau}, \tag{4}$$

in the steady state becomes

$$E\tau \propto \frac{1}{P_{\mathrm{o}}}, \tag{5}$$

where τ is the collision timescale and the inverse scaling of parallel ion flow speed with neutral pressure has been assumed based on our experimental results. Assuming a typical form for the collisional timescale, $\tau \propto 1/n\sigma v_{\mathrm{i}||}$, yields an electric field scaling of

$$E \propto \frac{1}{P_{\mathrm{o}}}. \tag{6}$$

In other words, the dependence of the parallel ion flow at the end of the helicon source on neutral pressure suggests that the double layer strength, i.e. potential difference across the layer, increases with decreasing pressure. This result is in contrast to observations of ion beam energies that are independent of neutral pressure in expanding hydrogen helicon plasmas [29] but consistent with a double layer strength that scales with the electron temperature (since, as is shown later, the electron temperature increases with decreasing neutral pressure in these experiments).

The plasma density, electron temperature, floating potential and plasma potential versus source neutral pressure measured at $z = 126$ cm in HELIX and $z = 188$ cm in LEIA are shown in figure 9. The floating potential measurements are referenced to the vacuum chamber, which is held at ground potential. The increase in plasma density with increasing neutral pressure is roughly linear, and the expansion chamber density is smaller than the source density by roughly one order of magnitude. In the plasma source, the electron temperature increases gradually from 5 to 6 eV as the neutral pressure drops below 2.5 mTorr and then increases sharply from 6 to 11 eV as the neutral pressure drops from 1.7 to 0.8 mTorr (figure 9(*b*)). The electron temperature in LEIA rises smoothly from 3.7 eV at a neutral pressure of 2.5 mTorr to 6.5 eV at a neutral pressure of 0.8 mTorr (figure 9(*f*)).

Although the most dramatic parameter variation occurs in the floating potential in the source (figure 9(*c*)), the physically important potential is the plasma potential (figure 9(*d*)). Based on equation (2), the plasma potential in the source decreases from roughly 40 V at 0.8 mTorr to 35 V at 1.7 mTorr: plasma potentials identical to those reported by Charles and Boswell [27] at the same neutral pressures in their helicon source. At the highest pressure investigated, the plasma potential in the source drops to approximately 30 V. The plasma potential in our expansion region is positive and smaller in magnitude, by approximately 15 V, than in the source for a neutral pressure of 1.7 mTorr. The more positive source plasma potential is consistent with acceleration of the ions out of the source and into LEIA.

A significant parallel ion flow is not observed in LEIA 38 cm beyond the helicon plasma source. The region from the end of the helicon source to 38 cm from the end of the source is not accessible with our existing LIF scanning probe. Measurements of parallel ion flow along the system axis in LEIA and HELIX at a source neutral pressure of 1.2 mTorr are shown in figure 10. Both the 38 cm long data gap and the large increase in parallel ion flow speed close to the end of the helicon source are evident in figure 10. In LEIA, only a single drifting ion population is observed. The drift speed in LEIA is comparable with the drift speed of the second, background, ion population observed at the end of the helicon source. There are two possible explanations for the apparent lack of parallel ion flow in LEIA. The first is that the ion flow speed decreases to subsonic velocities as the ions travel into the LEIA chamber. The second possibility is that the number of rapidly moving metastable ions that survive the 38 cm long trip into LEIA is too small to measure with our LIF apparatus.

Collisions with background neutrals or scattering arising from flow driven instabilities will reduce the velocity of energetic ions. Because the parallel ion temperatures in LEIA are much colder, $T_{\mathrm{i}||} \approx 0.1$ eV, than in HELIX, it is unlikely the ion flow is converted into random motion by ion scattering due to large amplitude waves, i.e. we would expect the ion temperature to increase as the parallel ion flow speed decreases. Collisions with background neutrals, whether charge-exchange or elastic collisions, will slow down energetic ions. The total momentum transfer cross section for Ar^+–Ar collisions, including charge-exchange and elastic collisions, at energies under 1 eV is relatively constant ($\langle\sigma\rangle \approx 1.3 \times 10^{-14}\,\mathrm{cm}^2$) [48] and yields an ion mean free path of $\lambda_{\mathrm{mfp}} = (2.2/P_{\mathrm{o}})$ cm, where P_{o} is the neutral pressure in milliTorr and the neutral gas is assumed to be at room temperature. For a source pressure of 1.2 mTorr, at which the data shown in figure 10 were obtained, the expansion chamber neutral pressure is 0.16 mTorr—yielding an ion mean free path of approximately 15 cm. This value is likely an underestimate of the collisional mean free path in this system as recent LIF measurements of neutral argon have demonstrated that the neutral density profile in the helicon source is hollow [49]. The hollow neutral density profile, as well as an axial neutral pressure gradient, in helicon sources arises from a combination of neutral pumping [50] and the high ionization fraction typical of helicon sources. Over a distance of 35 cm, exponential decay of the parallel ion flow speed due to an ion mean free path of 15 cm would drop the parallel ion flow speed from $9000\,\mathrm{m\,s^{-1}}$ to roughly $900\,\mathrm{m\,s^{-1}}$, consistent with the parallel ion flow speeds observed downstream of the helicon source at $z = 216$ cm, but flow measurements further downstream in LEIA are not consistent with a 15 cm mean free path.

Given that the LIF intensity measurements inside the helicon source appear to suggest that the bulk of the metastable ions in the helicon source are excited directly from the ion ground state, it is possible that a population of energetic electrons in the source is responsible for creation of the metastable ions required for LIF. When an electric double layer forms, there is a population of 'passing' ions, the ion beam, and a population of trapped electrons upstream of the double layer. Hints of such an electric beam in Langmuir probe I–V measurements have been reported in the other expanding helicon source double layer experiments [28]. In such a situation, energetic ions in the appropriate metastable state passing through the double layer can be depopulated collisionally, quenched, without a mechanism to

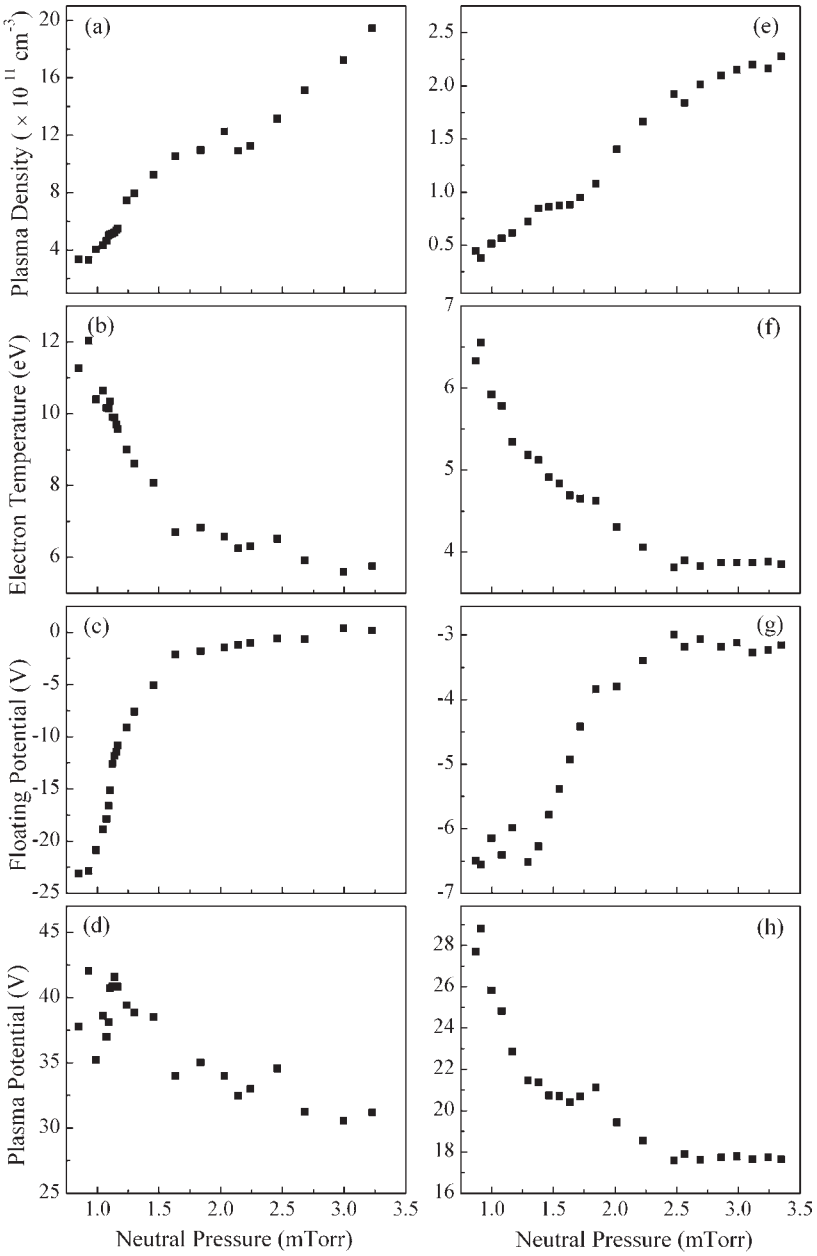

Figure 9. (*a*) Plasma density, (*b*) electron temperature, (*c*) floating potential and (*d*) plasma potential calculated from equation (2) at $z = 126$ cm in HELIX and (*e*) plasma density, (*f*) electron temperature, (*g*) floating potential and (*h*) plasma potential measured at $z = 188$ cm in LEIA versus neutral pressure in the helicon source for $B_{\mathrm{H}} = 730$ G, $B_{\mathrm{L}} = 34$ G, rf driving frequency of 9.5 MHz and rf power of 750 W.

easily repopulate those metastable states, i.e. the LIF signal for the ion beam will decrease exponentially with distance from the double layer. The quenching of the metastable ion states by collisions with neutrals, other ions and even electrons has been quantized in terms of a quenching cross section of $5 \pm 10^{-14}\,\mathrm{cm}^{-2}$ in the experiments of Cohen *et al* [30]: a value that is roughly a factor of two larger than previous estimates [51]. The corresponding mean free path of 5.2 cm yields a decrease in LIF intensity of 99.9% over 35 cm in LEIA. Thus, it is also possible that the absence of a significant ion flow in LEIA is an artefact of the LIF measurement process. In fact, in the experiments of Cohen *et al*, the average energy of the ion beam was observed to increase slightly with increasing distance from the double layer even though the LIF intensity from the ion beam decreased exponentially [30].

3.4. Effects of HELIX magnetic field strength

As a function of HELIX magnetic field, the parallel ion flow speed for four locations and parallel ion temperature for three locations in HELIX are shown in figures 11(*a*) and (*b*). In figures 11(*c*) and (*d*), the parallel ion flow speed and parallel ion temperature are shown for three locations along the axis in LEIA. The rf power was 750 W, the rf driving frequency was 9.5 MHz and the neutral pressure in the source was 1.2 mTorr, except for the parallel ion flow speed measurements at the end of the helicon source ($z = 146$ cm)

which were obtained at a neutral pressure of 1.5 mTorr. Consistent with the measurements made at a single value of source magnetic field strength shown in figures 6, 8 and 10, there is a clear axial gradient in parallel ion flow speed (figure 11(*a*)) and in parallel ion temperature (figure 11(*b*)) in the source. At all four locations, the parallel ion flow speed in the source is independent of the magnetic field strength, while the parallel ion temperature measured closest to the antenna, $z = 80$ cm, increases with source magnetic field strength. Further downstream, the parallel ion temperature is larger than at $z = 80$ cm, but the relative increase in parallel ion temperature with increasing source magnetic field strength is much smaller. Since both the parallel ion flow speed and parallel ion temperature increase with increasing distance from the antenna, it is likely that the observed ion heating results from thermalization of the ion flow, i.e. ion scattering converts a fraction of the flow energy into random motion.

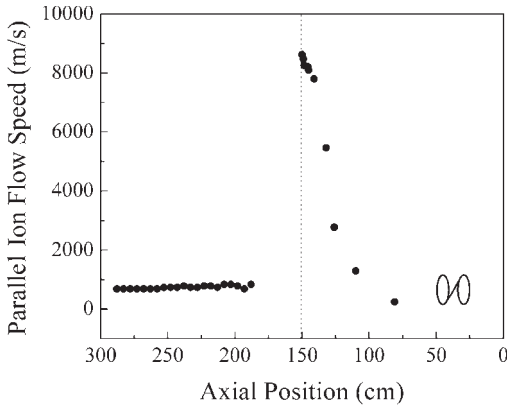

Figure 10. Parallel ion flow speed in HELIX and LEIA versus axial position for $B_H = 730$ G, $B_L = 34$ G, rf driving frequency of 9.5 MHz, rf power of 750 W and source neutral pressure of 1.2 mTorr. The vertical dashed line indicates the end of the helicon source, and the location of the rf antenna is also shown.

In LEIA, both the parallel ion flow speed (figure 11(*c*)) and parallel ion temperature (figure 11(*d*)) are independent of the HELIX magnetic field strength. Although the decrease in parallel flow of the slowly drifting single ion population in LEIA with increasing distance from the source antenna is difficult to see in figure 10, the expanded vertical axis scale of figure 11(*c*) provides a clearer picture of the drop in parallel ion flow speed as the ions travel into the LEIA chamber. In fact, a fit to the LEIA parallel ion flow data shown in figure 11(*c*) suggests that the mean free path for ions slowing down along the axis in LEIA is much greater than 35 cm, consistent with our previously stated hypothesis that the mean free path due to ion scattering by neutrals (charge-exchange and elastic scattering) may not explain completely the absence of the ion beam population in LEIA. Note also that the parallel ion temperatures in LEIA decrease with distance from the source to a roughly constant 0.08 eV. Such cooling of the ions is consistent with ion cooling by charge-exchange collisions. Temperatures of 0.08 eV are hotter than the neutral temperatures observed typically in the source [49] and suggest that the neutrals in LEIA may be hotter than in the source. Perhaps the most significant aspect of these LEIA flow measurements is that there is no evidence that the magnetic field ratio, i.e. the magnetic field expansion, has any effect on the flow speed of the single ion population observed in LEIA.

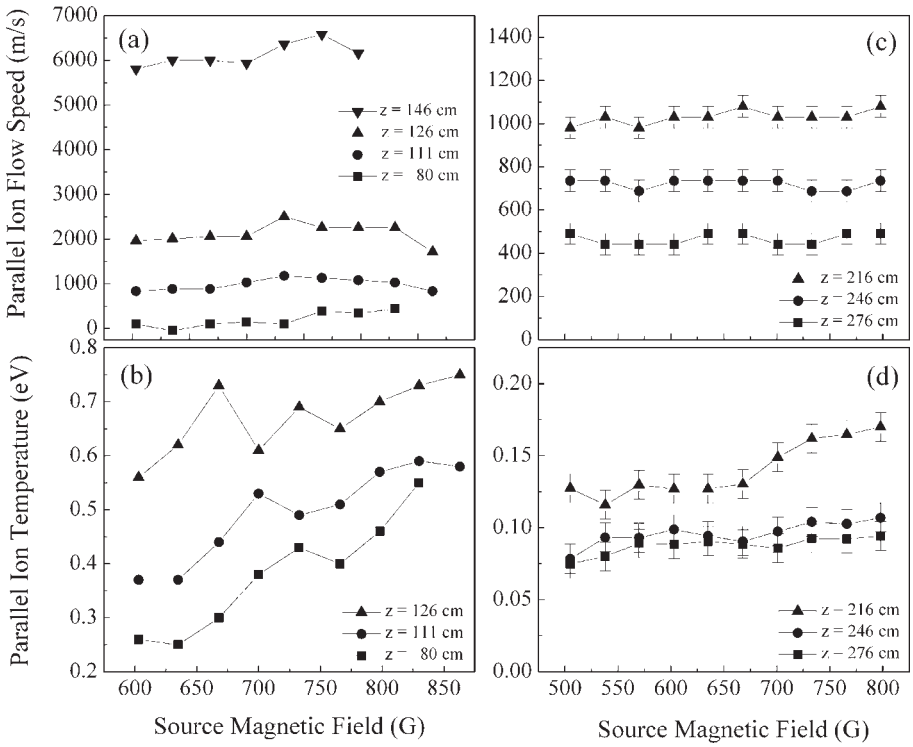

Figure 11. Parallel ion flow speed and parallel ion temperature measured at four locations in HELIX (*a*) and (*b*), respectively, and in LEIA (*c*) and (*d*), respectively, versus HELIX magnetic field strength for $B_L = 34$ G, rf driving frequency of 9.5 MHz, rf power of 750 W and a source neutral pressure of 1.2 mTorr, except for the $z = 146$ cm measurements in HELIX, which were obtained at a neutral pressure of 1.5 mTorr.

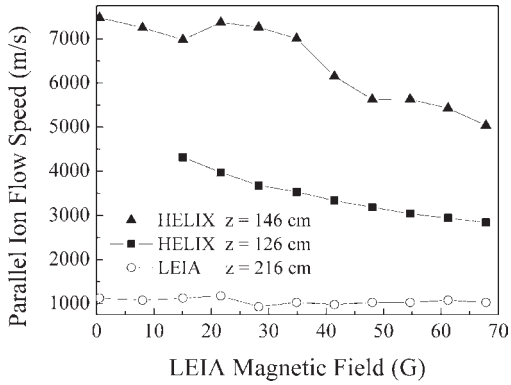

Figure 12. Parallel ion flow speed in HELIX at $z = 146$ cm (■) and $z = 126$ cm (▲) and in LEIA at $z = 216$ cm (○) for a HELIX magnetic field strength $B_H = 730$ G, rf driving frequency of 9.5 MHz, rf power of 750 W and a source neutral pressure of 1.1 mTorr.

3.5. Effects of LEIA magnetic field strength

The parallel ion flow speed in HELIX, at $z = 126$ cm and $z = 146$ cm, and in LEIA, at $z = 216$ cm, is shown in figure 12 as a function of LEIA magnetic field strength. For these measurements, the rf power was 750 W, the rf driving frequency was 9.5 MHz, the source magnetic field strength was 730 G and the neutral pressure in the source was 1.5 mTorr. Again, the parallel ion flow speed of the single ion population observed in LEIA is independent of the ratio of LEIA to HELIX magnetic field strengths. Decreasing the LEIA magnetic field strength from 65 to 10 G increases the parallel ion flow speed in HELIX at $z = 146$ cm from 5200 m s^{-1} to 7500 m s^{-1}, corresponding to an increase in ion energy from 5.3 to 11.1 eV.

According to *in situ* probe measurements made during the magnetic field strength scan from 65 to 10 G, the HELIX plasma density at $z = 126$ cm decreased by 20%, while the floating potential and electron temperature (and therefore the ion sound speed) in HELIX remained relatively constant. Thus, the parallel ion flow at the end of the source, $z = 146$ cm, is approximately equal to the ion sound speed at the smallest HELIX to LEIA magnetic field ratio (11.2) and increases to a little less than twice the sound speed at the largest value of the magnetic field ratio (73). Because the field expansion begins just inside the end of the helicon source (see figure 2), magnetic moment conservation, $\mu \equiv mv_\perp^2/2B = \text{constant}$, could play a role in accelerating the ions out of the source. Magnetic moment conservation predicts conversion of 85% of the perpendicular energy to parallel energy for a factor of 6.5 increase in magnetic field ratio, B_H/B_L. In this scan, the parallel kinetic ion energy at $z = 146$ cm in the source increases from 5.3 to 11.1 eV, and yet the parallel ion temperature is only 1 eV at the same location. For magnetic moment conservation to account for the observed ion acceleration, the perpendicular ion temperature at $z = 146$ cm (which we cannot measure) would have to be nearly 7 eV. Although we have observed significant ion temperature anisotropy in helicon sources [37], an anisotropy of 7 is many times larger than any we have observed in the source. Therefore, these parallel ion flow measurements suggest that the strength of the hypothesized double layer increases with increasing magnetic field ratio.

4. Conclusion

These measurements demonstrate that neutral pressure and, to a lesser extent, magnetic field geometry govern the acceleration of ions out of an open-ended helicon plasma source. Variations in rf driving frequency over the range 7.5–14 MHz and in the magnetic field strength in the helicon source over the range 600–900 G have a negligible effect on parallel ion flow speed in the helicon plasma source. A twofold increase in rf power (from 500 to 1000 W) yielded an increase in the flow speed by a factor of 1.7 (from 2600 to 4300 m s^{-1}), while a sevenfold decrease of the magnetic field strength in the expansion region (from 65 to 10 G) yielded an increase in parallel ion flow by a factor of 1.5 at the end of the helicon source (from 5200 to 7500 m s^{-1}).

The largest parallel ion flow speeds in the helicon source were observed at the lowest neutral pressure. As the neutral pressure was reduced from 1.4 to 1.1 mTorr, the ion flow speed increased from 5000 m s^{-1} ($\approx C_s$) to a supersonic speed of 8300 m s^{-1} ($\approx 1.7C_s$). Below a neutral pressure of 1.6 mTorr, two ion populations, a fast moving 'beam' and a slower moving background population, appeared at the end of the helicon source. The energy of the beam ions ($\sim$15 eV) is consistent with the 15 V difference in plasma potential between the helicon source and the expansion chamber. Given that two other groups investigating open-ended helicon sources reported recently a sharp increase in parallel flow speed below a threshold pressure [30] and formation of a weak double layer below a threshold pressure [27], this process of ion acceleration appears to be a characteristic of all such low-pressure, expanding helicon plasmas. Perhaps somewhat surprisingly, the ion acceleration process is common to these three experiments, even though the rf power densities of the sources differ significantly; one experiment employed a small, flux limiting aperture; our system includes a grounded metal chamber between the source and the region of expanding magnetic field; each experiment used a different rf antenna; and the plasma densities in the source all differed somewhat from each other. The dependence of the ion acceleration process on the neutral pressure suggests that there is probably a dimensionless scaling threshold for formation of the double layer common to all three experiments. In these experiments, the appearance of the second ion population corresponded to an ion mean free path to Debye length ratio of 500. If the requirement for double layer formation is that ions pass through the layer without collisions, these measurements suggest that the double layer may be 500 Debye lengths thick.

To further investigate the disappearance of the energetic ion population in the expansion chamber, we intend to measure the neutral velocity distribution function in the expansion chamber. Because it is possible that quenching of the metastable ions is responsible for the apparent elimination of the energetic ions, measurements of the neutral velocity distribution function will indicate whether or not there is significant momentum coupling to the neutrals—potentially an attractive characteristic of a helicon source based plasma propulsion system. We also intend to illuminate the expanding plasma with an electron beam of roughly 30 eV to repopulate the metastable ion states and determine if the energetic ions persist in the expansion region and are simply invisible to our LIF diagnostic.

Acknowledgments

We would like to thank the referees of this manuscript for some very helpful and insightful comments during the review process. This work was performed with support from National Science Foundation grant ATM-99988450 and the US Department of Energy under grant DE-FG02-97ER54420.

References

[1] Tanberg R 1930 *Phys. Rev*. **35** 1080
[2] Kobel E 1930 *Phys. Rev*. **36** 1636
[3] Gurevich A V, Pariiskaya L V and Pitaevskii L P 1966 *Sov. Phys.—JETP* **22** 449
[4] Eselevich V G and Fainshtein V G 1980 *Sov. Phys.—JETP* **52** 441
[5] Samir G, Wright K H and Stone N H 1982 *Rev. Geophys. Space Phys.* **21** 1631
[6] Hairapetian G and Stenzel R L 1988 *Phys. Rev. Lett.* **61** 1607
[7] Hairapetian G and Stenzel R L 1990 *Phys. Rev. Lett.* **65** 175
[8] Hairapetian G and Stenzel R L 1991 *Phys. Fluids* B **3** 899
[9] Wright K H, Stone, N H and Samir U 1985 *J. Plasma Phys.* **33** 71
[10] Wagli P and Donaldson T P 1978 *Phys. Rev. Lett.* **40** 875
[11] Singh N and Schunk R W 1983 *J. Geophys. Res.* **88** 7867
[12] Andersen S A, Jensen V O, Nielsen P and D'Angelo N 1969 *Phys. Fluids* **12** 557
[13] Korn P, Marshall T C and Schlesinger S P 1970 *Phys. Fluids* **13** 517
[14] Intrator T, Menard J and Hershkowitz N 1992 *Phys. Fluids* B **5** 806
[15] Coakley P and Hershkowitz N 1979 *Phys. Fluids* **22** 1171
[16] Charles C, Boswell R W and Porteus R K 1992 *J. Vac. Sci. Technol.* A **10** 398
[17] Charles C 1993 *J. Vac. Sci. Technol.* A **11** 157
[18] Charles C and Boswell R W 1995 *J. Vac. Sci. Technol.* A **13** 2067
[19] Chen F F, Jiang X and Evans J D 2000 *J. Vac. Sci. Technol.* A **18** 2108
[20] Perry A J and Boswell R W 1989 *Appl. Phys. Lett.* **55** 148
[21] Chang-Diaz F R *et al* 1999 *Fusion Technol*. **35** 243
[22] Squire J P, Chang Diaz F R, Glover T W, Jacobson V T, Chavers D G, Bengtson R D, Bering E A, Boswell R W, Goulding R H and Light M 2003 *Fusion Sci. Technol.* **43** 111
[23] Scheuer J T, Schoenberg K F, Gerwin R A, Hoyt R P, Henins I, Black D C, Mayo R M and Moses R W Jr 1994 *IEEE Trans. Plasma Sci.* **22** 1015
[24] Scime E E, Keiter P A, Balkey M M, Boivin R F, Kline J L, Blackburn M and Gary S P 2000 *Phys. Plasmas* **7** 2157
[25] Hussein M A and Emmert G A 1990 *J. Vac. Sci. Technol.* A **8** 2913
[26] Trevor D J, Sadeghi N, Nakano T, Derouard J, Gottscho R A, Pang Dow Foo and Cook J M 1990 *Appl. Phys. Lett.* **57** 1188
[27] Charles C and Boswell R W 2003 *Appl. Phys. Lett*. **82** 1356
[28] Charles C and Boswell R W 2004 *Phys. Plasmas* **11** 1706
[29] Charles C 2004 *Appl. Phys. Lett*. **84** 332
[30] Cohen S A, Siefert N S, Stange S, Boivin R F, Scime E E and Levinton F M 2003 *Phys. Plasmas* **7** 2593
[31] Boivin R F and Scime E E 2003 *Rev. Sci. Instrum*. **74** 4352
[32] Kline J L, Scime E, Boivin R F, Keesee A M and Sun X 2002 *Plasma Sources Sci. Technol.* **11** 413
[33] Sudit I D and Chen F F 1994 *Plasma Sources Sci. Technol.* **3** 162
[34] Scime E E, Boivin R F, Kline J L and Balkey M M 2002 *Rev. Sci. Instrum*. **72** 1672
[35] Stern R A and Johnson J A III 1975 *Phys. Rev. Lett.* **34** 1548
[36] Hill D H, Fornaca S and Wickham M G 1983 *Rev. Sci. Instrum.* **54** 309
[37] Scime E E, Keiter P A, Zintl M W, Balkey M M, Kline J L and Koepke M E 1998 *Plasma Sources Sci. Technol.* **7** 186
[38] Scime E E, Kline J L, Mathess D and Weber C II 2002 *Rev. Sci. Instrum*. **73** 1970
[39] Griem H R 1997 *Principles of Plasma Spectroscopy* (Cambridge: Cambridge University Press) p 160
[40] McWhirter R W P 1965 Spectral intensities *Plasma Diagnostics Techniques* (New York: Academic) ch 5, p 201
[41] Godyak V A, Piejak R B and Alexandrovich B M 2002 *Plasma Sources Sci. Technol.* **11** 525
[42] Chen F F 2003 *Mini-Course on Plasma Diagnostics* IEEE-ICOPS Meeting *(Jeju, Korea, June 5)*
[43] Lieberman M and Lichtenberg A 1994 *Principles of Plasma Discharges and Materials Processing* (New York: Wiley)
[44] Balkey M M, Boivin R F, Keiter P A, Kline J L and Scime E E 2001 *Plasma Sources Sci. Technol.* **10** 284
[45] Kline J L, Scime E E, Boivin R F, Keesee A M and Sun X 2002 *Phys. Rev. Lett*. **88** 195002
[46] Chen F F 1991 *Plasma Phys. Control. Fusion* **33** 339
[47] Keiter P A, Scime E E and Balkey M M 1997 *Phys. Plasmas* **4** 2741
[48] Phelps A V 1991 *J. Phys. Chem. Ref. Data* **20** 557
[49] Keesee A M, Scime E E, Biloiu C, Compton C, Hardin R A, Sun X and Boivin R 2003 *Bull. Am. Phys. Soc.* **48** 211
[50] Gilland J, Breun R and Hershkowitz N 1998 *Plasma Sources Sci. Technol*. **7** 416
[51] Skiff F, Bachet G and Doveil F 2001 *Phys. Plasmas* **8** 3139